Optimal consensus set for digital plane fitting

Rita Zrour, Yukiko Kenmochi, Hugues Talbot, Lilian Buzer, Yskandar Hamam, Ikuko Shimizu, Akihiro Sugimoto

Optimal consensus set for digital plane fitting

Rita Zrour[1], Yukiko Kenmochi[1], Hugues Talbot[1], Lilian Buzer[1], Yskandar Hamam[1,2]
[1]Université Paris-Est, LIGM, UPEMLV - ESIEE - CNRS, France
[2]F'SATI - Tshwane University of Technology, South Africa
{zrourr, y.kenmochi, h.talbot, l.buzer, y.hamam}@esiee.fr

Ikuko Shimizu
Tokyo University of Agriculture and Technology, Japan
ikuko@tuat.ac.jp

Akihiro Sugimoto
National Institute of Informatics, Japan
sugimoto@nii.ac.jp

Abstract

This paper presents a method for fitting a digital plane to a given set of points in a 3D image in the presence of outliers. We present a new method that uses a digital plane model rather than the conventional continuous model. We show that such a digital model allows us to efficiently examine all possible consensus sets and to guarantee the solution optimality and exactness. Our algorithm has a time complexity $O(N^3 \log N)$ together with a space complexity $O(N)$ where N is the number of points.

1. Introduction

Plane fitting is one of essential tasks in the field of 3D computer vision. For instance, this procedure is useful in image segmentation [10, 7], multi-view image registration [15, 2], as well as parameter fitting [6].

Several significant, optimal methods have been proposed in the literature, such as least-squares fitting, least-absolute-values fitting and least median of squares (LMS) [1, 6, 12]. In these methods, we use a continuous plane model that is defined by

$$\mathbf{P} = \{(x, y, z) \in \mathbb{R}^2 \ : \ ax + by + c + z = 0\}, \quad (1)$$

where $a, b, c \in \mathbb{R}$. The fitting is then carried out by optimizing different cost functions. For instance, least-squares minimizes the sum of geometric distances from all given points to the model. The solution can be obtained analytically, however it is very sensitive to the presence of outliers. Least-absolute-values fitting uses the L_1 norm, instead of the geometric distance, for its minimization. Some efficient iterative algorithms have been proposed for the fitting. However, they are still sensitive to outliers. In contrast, LMS minimizes the median of vertical/geometric distances of all given points to the model. Thus, the fitting is robust as long as the majority of given points are not outliers [14].

In this paper, we present a globally optimal method that, for a given arbitrary cloud of points, locates the planes minimizing the number of outliers, or equivalently maximizing the number of inliers, also called the consensus set. The idea of using such consensus sets were proposed in the RANdom SAmple Consensus (RANSAC) method [4], which is widely used in the field of computer vision. However RANSAC (and its variations) is inherently probabilistic in its approach, and does not deterministically guarantee the optimality of consensus sets. In contrast, our method is both deterministic and optimal.

In order to guarantee the optimality of consensus sets, we follow a digital geometry methodology [9] instead of the continuous model of (1). This methodology is arguably preferable if given all inputs are digital images. For instance, a digital model allows us to distinguish digitization-induced noise from actual noise produced by an image sensor. Related work using digital plane models can be found in [8, 13] for digital plane recognition, and shape polyhedrization [16] in both of the absence and presence of noise. However, to the best of our knowledge, outliers, namely points that do not fit the model, have never been dealt with in the field of digital geometry.

This work is an extension of our previous work on digital line fitting [17], but uses a significantly different method. Here, we show that, even though our digital plane fitting problem is 3D, we can treat it as a 2D problem by considering it in the dual space of the duality transform [3]. We show that our algorithm for digital plane fitting has a time complexity of $O(N^3 \log N)$, instead of $O(N^2 \log N)$ for digital line fitting, where N is the number of points, while the space complexity $O(N)$ is not affected by the dimension increase. We also point out that there are more degenerated cases for 3D than those for 2D, if our input data are all inte-

Preprint submitted to International Workshop on 3D Digital Imaging and Modeling, 3DIM 2009 June 2009

gers or rational numbers, which is often the case for digital images. We thus present a way to handle such degenerated cases with only simple modifications.

The rest of the paper is as follows: in section 2 we expose the framework of our digital model. In section 3 we prove the optimality of our result. In section 4 we provide an algorithm for the computation of the fit. Section 5 provides a method for extracting the parameters from the fit. Section 6 is devoted to results and applications. Section 7 states some conclusions and perspectives.

2. The problem of digital plane fitting

In this paper, we use a digital model, instead of the continuous one, for planes in a discrete space $\mathbb{Z}^3$ where $\mathbb{Z}$ is the set of all integers. We consider that using a digital model is natural when our input data is a digital image. In addition, we guarantee the optimal solution for our problem, as we mention in the next section.

A digital plane $\mathbf{D}(\mathbf{P})$ that is the digitization of $\mathbf{P}$ in (1) is defined by the set of discrete points satisfying two inequalities:

$$\mathbf{D}(\mathbf{P}) = \{(x, y, z) \in \mathbb{Z}^3 \ : \ 0 \leq ax+by+z+c \leq w\} \quad (2)$$

where w is a given constant value. Geometrically, $\mathbf{D}(\mathbf{P})$ is a set of discrete points lying between two parallel planes $ax + by + z + c = 0$ and $ax + by + z + c = w$, and w specifies the vertical distance between them. From the digital geometrical point of view [9], w should not be less than 1 if we expect that $\mathbf{D}(\mathbf{P})$ is 18-connected. More precisely, in order to keep the connectivity with the minimum distance, we need to consider the distance w not only in the z-axis direction as shown in (2) but also in the x- and y-axis directions. For digital planes $\mathbf{D}(\mathbf{P})$ with the distance w in the other directions, we simply make the permutation of x, y and z in (2), and put the constraints, $-1 \leq a \leq 1$, $-1 \leq b \leq 1$. Hereafter, discussions will be made by using (2), since they are also valid for the other models.

Using the above digital plane model, our fitting problem is then described as follows: given a finite set of discrete points,

$$\mathbf{S} = \{\boldsymbol{x_i} \in \mathbb{Z}^3 \ : \ i = 1, 2, \ldots, N\},$$

we would like to find a digital plane $\mathbf{D}(\mathbf{P})$ such that $\mathbf{D}(\mathbf{P})$ contains the maximum number of points in $\mathbf{S}$. Points $\boldsymbol{x} \in \mathbf{S}$ are called inliers if $\boldsymbol{x} \in \mathbf{S} \cap \mathbf{D}(\mathbf{P})$; otherwise, they are called outliers.

3. Digital planes and their consensus sets

In this section, we show an important property of inlier sets, also called consensus sets, of digital planes. Our algorithm presented in the next section is based on this property. Since the size of $\mathbf{S}$ is finite and each element $\boldsymbol{x} \in \mathbf{S}$ has finite coordinates, we notice that the number of different consensus sets for a digital plane fitting of $\mathbf{S}$ is finite as well. Thus, if we can find all different consensus sets $\mathbf{C}$ from a given $\mathbf{S}$, we just verify the size of each $\mathbf{C}$ to find the maximum one (ones if there are several) as the optimal solution. In the following, we will show that it is possible.

Before presenting the main proposition, we give some notions related to digital planes. The two parallel planes that are given by the equations (2) are called the support planes of a digital plane. Discrete points that are on support planes are called critical points of a digital plane.

Proposition 1. *Let $\mathbf{C}$ be a consensus set of $\mathbf{S}$ for a digital plane. It is possible to find a new digital plane whose consensus set is the same as $\mathbf{C}$ such that it has at least three critical points.*

Proof. Let $\mathbf{D}$ be an initial digital plane that contains all points in $\mathbf{C}$ as its inliers. Then, the following four cases can be considered when observing the critical points of $\mathbf{D}$.
(1) Suppose that $\mathbf{D}$ has more than two critical points, then the proposition is correct in this case.
(2) Suppose that $\mathbf{D}$ has two critical points $\boldsymbol{p}_1$ and $\boldsymbol{p}_2$. $\boldsymbol{p}_1$ and $\boldsymbol{p}_2$ may be located on one side or either side of the two parallel support planes of $\mathbf{D}$ as illustrated in Figures 1 (a) or 2 (a), respectively. First, we take the projections $\boldsymbol{p}'_1$ (resp. $\boldsymbol{p}'_2$) of $\boldsymbol{p}_1$ (resp. $\boldsymbol{p}_2$) on the other support plane where $\boldsymbol{p}_1$ (resp. $\boldsymbol{p}_2$) does not exist in the z-axis direction. We then apply a rotation to $\mathbf{D}$ in such a way as to maintain the distance w between the support planes until finding another point $\boldsymbol{p}_3$ in $\mathbf{C}$ so that $\boldsymbol{p}_3$ becomes a critical point. To achieve this, in the illustrative case of Figure 1 (a), to the support plane where $\boldsymbol{p}_1$ and $\boldsymbol{p}_2$ exist, we apply a rotation around the line going through $\boldsymbol{p}_1$ and $\boldsymbol{p}_2$, as illustrated in Figures 1 (b). To the other support plane, we apply a rotation around the line going through $\boldsymbol{p}'_1$ and $\boldsymbol{p}'_2$, as illustrated in Figures 1 (b). In the case of Figure 2 (a), similarly, to the support plane where $\boldsymbol{p}_1$ (resp. $\boldsymbol{p}_2$) exists, we apply a rotation around the line going through $\boldsymbol{p}_1$ and $\boldsymbol{p}'_2$ (resp. $\boldsymbol{p}'_1$ and $\boldsymbol{p}_2$), as illustrated in Figures 2 (b). Note that we can rotate $\mathbf{D}$ either clockwise or counterclockwise.
(3) Suppose that $\mathbf{D}$ has one critical point $\boldsymbol{p}_1$ as illustrated in Figure 3 (a). In this case, we also consider the projection of $\boldsymbol{p}_1$, $\boldsymbol{p}'_1$. We then apply a rotation to each support plane until finding another point $\boldsymbol{p}_2$ in $\mathbf{C}$ so that $\boldsymbol{p}_2$ becomes a critical point, as illustrated in Figure 3 (b). The support plane where $\boldsymbol{p}_1$ (resp. $\boldsymbol{p}'_1$) exists is rotated around any line going through $\boldsymbol{p}_1$ (resp. $\boldsymbol{p}'_1$) on the support plane. If just one point $\boldsymbol{p}_2$ is found as a second critical point after the rotation, then another rotation is made, as mentioned in the previous case, in order to obtain a third critical point $\boldsymbol{p}_3$.
(4) Suppose that $\mathbf{D}$ has no critical point as illustrated in Figure 4 (a). In this case, we first apply a translation to $\mathbf{D}$ in

order to find a first critical point $\boldsymbol{p}_1$. Note that a translation can be made in any direction while the two support planes maintain a constant distance w between them. During such a translation, if more than two points are found as critical points, then the proof is complete. If just one point $\boldsymbol{p}_1$ is found, as illustrated in Figure 4 (b), then a rotation is made as mentioned in the previous case, in order to obtain a second critical point $\boldsymbol{p}_2$. If during this rotation just one point $\boldsymbol{p}_2$ is detected, then another rotation is accomplished in order to detect a third critical point $\boldsymbol{p}_3$ as described in the first case. □

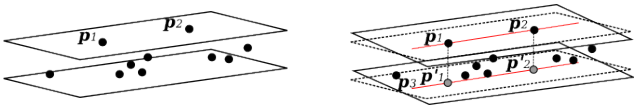

(a) (b)

Figure 1. A digital plane that has two critical points $\boldsymbol{p}_1$ and $\boldsymbol{p}_2$ on one of its support planes (a), and its rotated digital plane that also has a third critical point $\boldsymbol{p}_3$ (b).

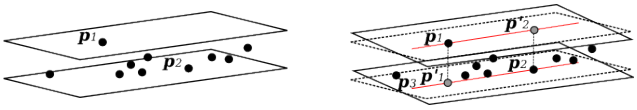

(a) (b)

Figure 2. A digital plane that has two critical points $\boldsymbol{p}_1$ and $\boldsymbol{p}_2$ on distinct support planes (a), and its rotated digital plane that also a the third critical point $\boldsymbol{p}_3$ (b).

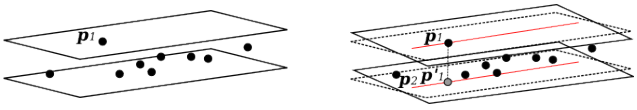

(a) (b)

Figure 3. A digital plane that has one critical point $\boldsymbol{p}_1$ (a), and its rotated digital plane that also has a second critical point $\boldsymbol{p}_2$ (b).

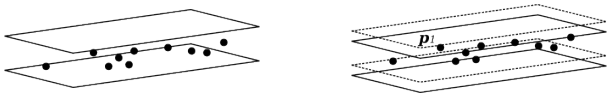

(a) (b)

Figure 4. A digital plane that has no critical point (a), and its translated digital plane that has one critical point $\boldsymbol{p}_1$ (b).

From this proposition, we see that we can find a digital plane $\mathbf{D}(\mathbf{P})$ for any consensus set $\mathbf{C}$ of $\mathbf{S}$ such that it has at least three critical points. This is intuitively understandable, because when we move a digital plane $\mathbf{D}(\mathbf{P})$ in the space, its consensus set $\mathbf{C}$ will be changed the moment that a critical point goes out from $\mathbf{D}(\mathbf{P})$, namely, becomes an outlier, due to the motion. Indeed, such a digital plane $\mathbf{D}(\mathbf{P})$ can be constructed from a triplet of points chosen from $\mathbf{S}$ such that they become critical points of $\mathbf{D}(\mathbf{P})$. Consequently, we can find all $\mathbf{C}$ from those $\mathbf{D}(\mathbf{P})$ constructed from all possible triplets of points in $\mathbf{S}$. Note that there are at most eight different $\mathbf{D}(\mathbf{P})$ constructed from each triplet of points in $\mathbf{S}$.

4. Digital plane fitting algorithm

A naive algorithm for 3D digital plane fitting derived from Proposition 1 is to make the consensus set $\mathbf{C}$ for each triplet of points in $\mathbf{S}$ and to verify the size of $\mathbf{C}$ for obtaining the maximum one among all triplets. Thus, such an algorithm has a $O(N^4)$ time complexity. In this section, we will present a new algorithm that has a less complexity.

Our algorithm is based on a similar idea to the one for 2D digital line fitting, presented in [17]. The key idea for the extension to 3D digital plane fitting is treating the 3D problem as a 2D problem. We first show how to reduce the dimension from three to two, and then obtain an algorithm providing a $O(N^3 \log N)$ time and $O(N)$ space complexity.

We first describe the digital plane fitting problem in the dual space of the duality transform, because our algorithm works in the dual space of the duality transform [3], similarly to the 2D digital line fitting. We then present an algorithm to exhibit the optimal consensus set (sets if there are several) that maximizes the number of inliers of a fitted digital plane from a given set $\mathbf{S}$ of discrete points in 3D, step by step. We also describe special treatments for degenerated cases; it should be noted that digital images likely present many degenerated cases that must be processed separately.

4.1. Digital plane fitting in the dual space

A point $\boldsymbol{p} = (x, y, z)$ in the primal space associates to a non-vertical plane

$$P_{\boldsymbol{p}} = \{(a, b, c) : xa + yb + c + z = 0\} \tag{3}$$

in the dual space. Conversely, a non-vertical plane in the primal space associates to a point in the dual space. Because a digital plane defined by (2) is regarded as a set of non-vertical parallel planes whose normal vectors are $(a, b, 1)$ and whose z-intercepts are between $-c$ and $w - c$, it forms a vertical line segment of length w in the dual space as illustrated in Figure 5. Since all points of $\mathbf{S}$ in the primal space are represented by planes in the dual space, our problem of finding the optimal consensus set for digital plane fitting in the primal space is equivalent to searching the best position of the vertical line segment of length w such that it intersects with the maximum number of planes in the dual space.

We now need a search procedure for an optimal segment. Thanks to Proposition 1, we know that, for any consensus set, there exists a digital plane featuring at least three critical points, among which at least two are on one of the support planes. Thus, taking two different points $\boldsymbol{p}$, $\boldsymbol{q}$ from $\mathbf{S}$ in the primal space, we first consider all the digital planes on

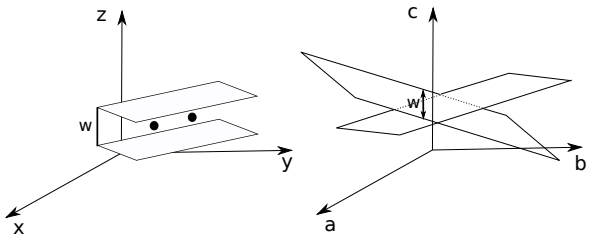

Figure 5. A digital plane in the primal space (left) corresponds to a vertical line segment of length w in the dual space (right).

which both $\boldsymbol{p}$ and $\boldsymbol{q}$ are critical points on the same support plane. In the dual space, digital planes having two critical points $\boldsymbol{p}$, $\boldsymbol{q}$ forms two strips, which will be described in Section 4.2. In Section 4.3, we explain how digital planes with two critical points $\boldsymbol{p}$, $\boldsymbol{q}$ appear in the strips when they have a third critical point $\boldsymbol{r}$. In Section 4.4, we then show how to obtain the maximum number of inliers and its digital plane parameters in the strips.

4.2. Strips made from a critical point pair

Let $\boldsymbol{p} = (x_{\boldsymbol{p}}, y_{\boldsymbol{p}}, z_{\boldsymbol{p}})$ and $\boldsymbol{q} = (x_{\boldsymbol{q}}, y_{\boldsymbol{q}}, z_{\boldsymbol{q}})$. In the dual space, they represent two planes $P_{\boldsymbol{p}}$ and $P_{\boldsymbol{q}}$, defined by (3). They intersect in a line $L^0_{\boldsymbol{pq}}$ if $\boldsymbol{p}$ and $\boldsymbol{q}$ are chosen such that $(x_{\boldsymbol{p}} - x_{\boldsymbol{q}})^2 + (y_{\boldsymbol{p}} - y_{\boldsymbol{q}})^2 \neq 0$; otherwise, $P_{\boldsymbol{p}}$ and $P_{\boldsymbol{q}}$ are parallel, and no intersection line can be found. The intersection line $L^0_{\boldsymbol{pq}}$ is represented by the following equation:

$$L^0_{\boldsymbol{pq}} = \{\boldsymbol{v} = (a, b, c) : \boldsymbol{v} = \boldsymbol{u} + t\boldsymbol{d}, t \in \mathbb{R}\}$$

where

$$\begin{aligned} \boldsymbol{d} &= (x_{\boldsymbol{p}}, y_{\boldsymbol{p}}, 1) \wedge (x_{\boldsymbol{q}}, y_{\boldsymbol{q}}, 1) \\ &= (y_{\boldsymbol{p}} - y_{\boldsymbol{q}}, x_{\boldsymbol{q}} - x_{\boldsymbol{p}}, x_{\boldsymbol{p}} y_{\boldsymbol{q}} - x_{\boldsymbol{q}} y_{\boldsymbol{p}}), \end{aligned}$$

and $\boldsymbol{u} = (u_a, u_b, u_c)$; $\boldsymbol{u}$ is a chosen point on $L^0_{\boldsymbol{pq}}$. For example, if $x_{\boldsymbol{p}} y_{\boldsymbol{q}} \neq x_{\boldsymbol{q}} y_{\boldsymbol{p}}$, by fixing $u_c = 0$, u_a and u_b are automatically found since $\boldsymbol{u}$ is on both $P_{\boldsymbol{p}}$ and $P_{\boldsymbol{q}}$.

Once $L^0_{\boldsymbol{pq}}$ is found, then, all the digital planes on which both $\boldsymbol{p}$ and $\boldsymbol{q}$ are critical points on the same support plane in the primal space correspond to the set of all the vertical line segments of length w having one of its endpoints on $L^0_{\boldsymbol{pq}}$ in the dual space, as shown in Figure 6. We see in the figure that the set of such digital planes, therefore, forms two strips in the plane $Q_{\boldsymbol{pq}}$ that contains $L^0_{\boldsymbol{pq}}$ and the direction parallel to the c-axis. Taking the d-axis in $Q_{\boldsymbol{pq}}$ as the orthogonal one to the c-axis, such $Q_{\boldsymbol{pq}}$ is illustrated in Figures 6 and 7. Each strip on $Q_{\boldsymbol{pq}}$ illustrated in Figure 7 is bounded by two parallel lines, $L^0_{\boldsymbol{pq}}$ and $L^i_{\boldsymbol{pq}}$ for $i = 1, 2$, which are represented by:

$$\begin{aligned} L^1_{\boldsymbol{pq}} &= \{\boldsymbol{v} = (a, b, c) : \boldsymbol{v} = \boldsymbol{u} + \boldsymbol{e} + t\boldsymbol{d}, t \in \mathbb{R}\}, \\ L^2_{\boldsymbol{pq}} &= \{\boldsymbol{v} = (a, b, c) : \boldsymbol{v} = \boldsymbol{u} - \boldsymbol{e} + t\boldsymbol{d}, t \in \mathbb{R}\}, \end{aligned}$$

where $\boldsymbol{e} = (0, 0, 1)$.

4.3. Digital planes with a critical point triplet

Hereafter, we focus on one of the strips in $Q_{\boldsymbol{pq}}$, because the following discussion is valid for both strips. Let us consider the strip bounded by $L^0_{\boldsymbol{pq}}$ and $L^1_{\boldsymbol{pq}}$, as illustrated in Figure 7. According to Proposition 1, we choose a point $\boldsymbol{r} \in \mathbf{S} \setminus \{\boldsymbol{p}, \boldsymbol{q}\}$ to be the third critical point of a fitted digital plane such that $\boldsymbol{r}$ is not colinear with $\boldsymbol{p}$ and $\boldsymbol{q}$; the colinear case will be handled separately as a degenerated case in Section 4.6. Any point $\boldsymbol{r}$ in the primal space is represented by the line $L_{\boldsymbol{r}}$ in $Q_{\boldsymbol{pq}}$ in the dual space, which is the intersection between $P_{\boldsymbol{r}}$ and $Q_{\boldsymbol{pq}}$, as shown in Figure 7. We see in this figure that $L_{\boldsymbol{r}}$ intersects each of the strip boundaries, $L^0_{\boldsymbol{pq}}$ and $L^1_{\boldsymbol{pq}}$, if it is not parallel to $L^0_{\boldsymbol{pq}}$; the parallel case will be also dealt with separately as a degenerated case in Section 4.6. The intersections between $L_{\boldsymbol{r}}$ and $L^i_{\boldsymbol{pq}}$, $\sigma^i_{\boldsymbol{r}} = (a^i_{\boldsymbol{r}}, b^i_{\boldsymbol{r}}, c^i_{\boldsymbol{r}})$, for $i = 0, 1$, are calculated from $L^i_{\boldsymbol{pq}}$ and $P_{\boldsymbol{r}}$. Geometrically, the vertical line segment in the strip, one of whose endpoints is one of the intersections $\sigma^i_{\boldsymbol{r}}$, in the dual space corresponds to a digital plane with three

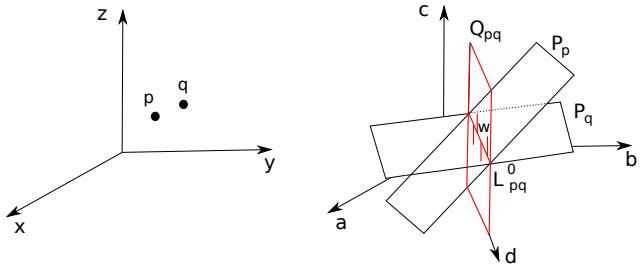

Figure 6. All the digital planes with two critical points $\boldsymbol{p}$ and $\boldsymbol{q}$ in the primal space (left) correspond to a set of vertical line segments of length w having one of its endpoints on the intersection line of the two planes $P_{\boldsymbol{p}}$ and $P_{\boldsymbol{q}}$ (right).

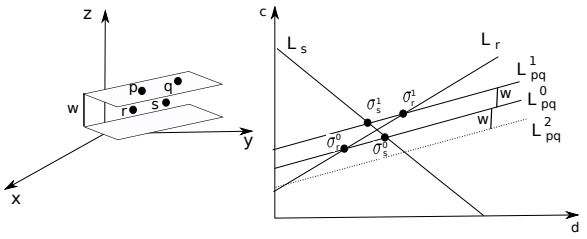

Figure 7. Four points $\boldsymbol{p}$, $\boldsymbol{q}$, $\boldsymbol{r}$ and $\boldsymbol{s}$ in the primal space (left), and their interpretations in the cross-section $Q_{\boldsymbol{pq}}$ of the dual space (right). $Q_{\boldsymbol{pq}}$ is made as the plane that contains the intersection line $L^0_{\boldsymbol{pq}}$ of $P_{\boldsymbol{p}}$ and $P_{\boldsymbol{q}}$ and the parallel direction to the c-axis, as illustrated in Figure 6. In $Q_{\boldsymbol{pq}}$, all the digital planes having $\boldsymbol{p}$ and $\boldsymbol{q}$ as critical points are represented by the strips each of which is bounded by $L^0_{\boldsymbol{pq}}$ and either of its parallel lines $L^1_{\boldsymbol{pq}}$ and $L^2_{\boldsymbol{pq}}$. The other points $\boldsymbol{r}$ and $\boldsymbol{s}$ in the primal space are represented by the two lines $L_{\boldsymbol{r}}$ and $L_{\boldsymbol{s}}$ in $Q_{\boldsymbol{pq}}$.

critical points $\boldsymbol{p}$, $\boldsymbol{q}$ and $\boldsymbol{r}$ in the primal space. This indicates that the digital planes corresponding to the vertical line segments between the two intersections $\sigma^0_{\boldsymbol{r}}$ and $\sigma^1_{\boldsymbol{r}}$ in the strip always contain $\boldsymbol{r}$ as an inlier.

4.4. Finding the largest consensus set in a strip

In order to know the number of inliers within the digital planes with two critical points $\boldsymbol{p}$ and $\boldsymbol{q}$, we check the intersections $\sigma^0_{\boldsymbol{r}}$ and $\sigma^1_{\boldsymbol{r}}$ of $L_{\boldsymbol{r}}$ for all $\boldsymbol{r} \in \mathbf{S}\backslash\{\boldsymbol{p},\boldsymbol{q}\}$ with the strip boundaries, $L^0_{\boldsymbol{pq}}$ and $L^1_{\boldsymbol{pq}}$. We use a function $f^i_{\boldsymbol{r}}$, for $i = 0, 1$, which is set to be 1 if $L_{\boldsymbol{r}}$ enters the strip from $L^i_{\boldsymbol{pq}}$, and -1 if $L_{\boldsymbol{r}}$ leaves the strip from $L^i_{\boldsymbol{pq}}$.

Once the intersections $\sigma^i_{\boldsymbol{r}} = (a^i_{\boldsymbol{r}}, b^i_{\boldsymbol{r}}, c^i_{\boldsymbol{r}})$, and the associated function $f^i_{\boldsymbol{r}}$ for $i = 0, 1$ are calculated for all $\boldsymbol{r} \in \mathbf{S} \setminus \{\boldsymbol{p},\boldsymbol{q}\}$, we sort all the quadruples $(a^i_{\boldsymbol{r}}, b^i_{\boldsymbol{r}}, c^i_{\boldsymbol{r}}, f^i_{\boldsymbol{r}})$ in increasing order by using either $a^i_{\boldsymbol{r}}$ or $b^i_{\boldsymbol{r}}$ as keys; if $Q_{\boldsymbol{pq}}$ is not perpendicular to the a-axis, we use $a^i_{\boldsymbol{r}}$; otherwise, we use $b^i_{\boldsymbol{r}}$. As for determining the location of the maximum number of inliers, another function $F(a)$ (resp. $F(b)$, depending on the key selection) is used; after initially setting $F(a) = 2$ for every a, since we already know that $\boldsymbol{p}$ and $\boldsymbol{q}$ are inliers, then the value $f^i_{\boldsymbol{r}}$ is added to $F(a)$ in the above sorted order. By looking for the maximum value of the function $F(a)$, we obtain the parameter set (a, b, c) corresponding to the maximum optimal consensus set for a pair of critical points $\boldsymbol{p}$ and $\boldsymbol{q}$. In this section, we consider that all $L_{\boldsymbol{r}}$ enter or leave a strip at different moments. The degenerated cases such that many lines $L_{\boldsymbol{r}}$ enter or leave a strip at the same moment will be described in Section 4.6.

4.5. Algorithm

We now present Algorithm 1. Input is a set $\mathbf{S}$ of discrete points and a distance value w of our digital plane model. Output is a set $\mathbf{V}$ of parameter values $(a^{\mathbf{c}}, b^{\mathbf{c}}, c^{\mathbf{c}})$ corresponding to the fitted digital planes of that give the optimal consensus sets. In the algorithm, we consider another strip bounded by $L^0_{\boldsymbol{pq}}$ and $L^2_{\boldsymbol{pq}}$ in Steps 5, 11 and 25.

We remark that, because $c^i_{\boldsymbol{r}}$ is not used for the sorting step and can be calculated from $a^i_{\boldsymbol{r}}$ and $b^i_{\boldsymbol{r}}$, we do not have to store it for each intersection. Simply for a candidate of the optimal consensus set, we calculate it as shown in Steps 26 and 28. Note that, depending on the strip, we calculate different $c^{\mathbf{c}}$ because of the translation difference w between the two strips.

In Steps 13 and 19, we only show the case where a_k is used as keys for sorting. However, if $Q_{\boldsymbol{pq}}$ is perpendicular to the a-axis, all a_k has the same value. In such a case, as mentioned above, we use b_k as keys, instead of a_k.

The time complexity of the algorithm is $O(N^3 \log N)$, because we have N points in $\mathbf{S}$ and each pair of $\boldsymbol{p}$ and $\boldsymbol{q}$ in $\mathbf{S}$ needs the complexity $O(N \log N)$ for sorting at most $2N - 4$ different values $a^i_{\boldsymbol{r}}$ for $\boldsymbol{r} \in \mathbf{S} \setminus \{\boldsymbol{p},\boldsymbol{q}\}$ and $i = 0, 1$. The space complexity is $O(N)$ because for each sorting we have at most $2N - 4$ different triplets (a_k, b_k, f_k).

Because all inputs can be given as integers or rational numbers, all computations in Algorithm 1 can be performed using only rational numbers. This ensures that all results obtained by Algorithm 1 contain no calculation error. However, degenerated cases may occur, which will be discussed

Algorithm 1: Digital plane fitting

input : A set $\mathbf{S}$ of N discrete points, a distance w
output: A set $\mathbf{V}$ of parameter value triplets $(a^{\mathbf{c}}, b^{\mathbf{c}}, c^{\mathbf{c}})$ of the best fitted digital planes

1 **begin**
2 initialize $Max = 0$;
3 **foreach** $\{\boldsymbol{p},\boldsymbol{q}\} \in \mathbf{S}$ **do**
4 calculate $L^0_{\boldsymbol{pq}}$;
5 **for** $l = 1, 2$ **do**
6 initialize $F = 2$;
7 initialize the array $T[k]$ for $k = 1, \ldots, 2N - 4$;
8 set $j = 0$;
9 **foreach** $\boldsymbol{r} \in \mathbf{S} \setminus \{\boldsymbol{p},\boldsymbol{q}\}$ **do**
10 calculate $a^i_{\boldsymbol{r}}$ and $b^i_{\boldsymbol{r}}$ for $i = 0, 1$;
11 **if** $l = 2$ **then**
12 calculate $a^2_{\boldsymbol{r}}$ and $b^2_{\boldsymbol{r}}$ and reset $a^1_{\boldsymbol{r}} = a^2_{\boldsymbol{r}}$ and $b^1_{\boldsymbol{r}} = b^2_{\boldsymbol{r}}$;
13 **if** $a^0_{\boldsymbol{r}} < a^1_{\boldsymbol{r}}$ **then**
14 set $f^0_{\boldsymbol{r}} = 1$, $f^1_{\boldsymbol{r}} = -1$;
15 **else**
16 set $f^0_{\boldsymbol{r}} = -1$, $f^1_{\boldsymbol{r}} = 1$;
17 set the tuple, $(a^i_{\boldsymbol{r}}, b^i_{\boldsymbol{r}}, f^i_{\boldsymbol{r}})$, for $i = 0, 1$, in $T[2j + i]$;
18 $j = j + 1$;
19 sort all the tuple elements (a_k, b_k, f_k) for $k = 1, \ldots, 2j$ in T with a_k as keys;
20 **for** $k = 1, \ldots, 2j$ **do**
21 $F = F + f_k$;
22 **if** $F > Max$ **then** set $Max = F$, $\mathbf{V} = \emptyset$;
23 **if** $F = Max$ **then**
24 set $a^{\mathbf{c}} = a_k$, $b^{\mathbf{c}} = b_k$;
25 **if** $l = 1$ **then**
26 $c^{\mathbf{c}} = -a_k x_{\boldsymbol{p}} - b_k y_{\boldsymbol{p}} - z_{\boldsymbol{p}}$;
27 **else**
28 $c^{\mathbf{c}} = -a_k x_{\boldsymbol{p}} - b_k y_{\boldsymbol{p}} - z_{\boldsymbol{p}} + w$;
29 put $(a^{\mathbf{c}}, b^{\mathbf{c}}, c^{\mathbf{c}})$ in $\mathbf{V}$;
30 return $\mathbf{V}$;
31 **end**

in the followings.

4.6. Degenerated cases

In this section, we explain how we can deal with degenerated cases, which are not considered in Algorithm 1. The following three cases are summarized.

First, if three points $\boldsymbol{p}$, $\boldsymbol{q}$ and $\boldsymbol{r}$ are colinear in the primal space, their associated planes $P_{\boldsymbol{p}}$, $P_{\boldsymbol{q}}$ and $P_{\boldsymbol{r}}$ have a line intersection in the dual space. Therefore, for any digital plane having $\boldsymbol{p}$ and $\boldsymbol{q}$ as its critical points also has $\boldsymbol{r}$ as its another critical point. Thus, the function $F(a)$ initially set to 2 for the inclusion of $\boldsymbol{p}$ and $\boldsymbol{q}$ as inliers will be automatically increased by 1 because of the inclusion of $\boldsymbol{r}$.

Secondly, suppose that $\boldsymbol{p}$, $\boldsymbol{q}$ and $\boldsymbol{r}$ are not colinear, but there is no intersection between $L^0_{\boldsymbol{pq}}$ and $L_{\boldsymbol{r}}$ in $Q_{\boldsymbol{pq}}$; $L_{\boldsymbol{r}}$ is parallel to $L^0_{\boldsymbol{pq}}$. If $L_{\boldsymbol{r}}$ is between $L^0_{\boldsymbol{pq}}$ and $L^1_{\boldsymbol{pq}}$ (resp. $L^2_{\boldsymbol{pq}}$), then we set the initial value of the function $F(a)$ to 3 when $l = 1$ (resp. $l = 2$) because $\boldsymbol{r}$ is an inlier for any a. Otherwise, we set it to 2, as described in Algorithm 1, because $\boldsymbol{r}$ is an outlier for any a.

Lastly, when many lines $L_{\boldsymbol{r}}$ enter or leave a strip at the same moment a, all the positive valued $f^i_{\boldsymbol{r}}$ of that moment must be added to the function $F(a)$ at once (Step 21 in Algorithm 1), and the value $F(a)$ is compared with the current maximum value Max (Step 22 in Algorithm 1). Note that all the negative valued $f^i_{\boldsymbol{r}}$ of the same moment a must be added after the comparison to the value $F(a)$. Indeed such a point $\boldsymbol{r}$ must be considered as an inlier until that moment.

5. Feasible digital plane parameters

Once an optimal consensus set $\mathbf{C}$ for digital plane fitting to a given point set $\mathbf{S}$ is found, we need the corresponding digital plane parameters in most applications. A continuous plane model such as (1) can be used to estimate them, for example, by applying the least squared method [6] to $\mathbf{C}$. However, one must be careful because this may modify the inlier set. In such a case, a new $\mathbf{C}$ must be recalculated from a new estimated plane, leading to an inefficient iterative procedure.

In our case, however, since we use the digital plane model of (2) instead of (1), we do not need such an estimation method, and there is no danger or changing the inlier set. We can obtain all feasible solutions for the parameters of digital planes fitted to an obtained optimal $\mathbf{C}$ by simply looking for all feasible solutions (a, b, c) that satisfy the inequalities of (2) for all $(x, y, z) \in \mathbf{C}$.

Such feasible solutions of digital planes are called preimages [5]. In contrast to the preimages of digital lines in 2D, the structure of the preimages of digital planes is not simple; we even do not know the maximum number of vertices or facets of a convex polyhedron, that constitutes a preimage of a digital plane. Further study is necessary.

6. Experiments

For our experiments, we applied our proposed method to two example data, such as a 3D discrete point cloud and a

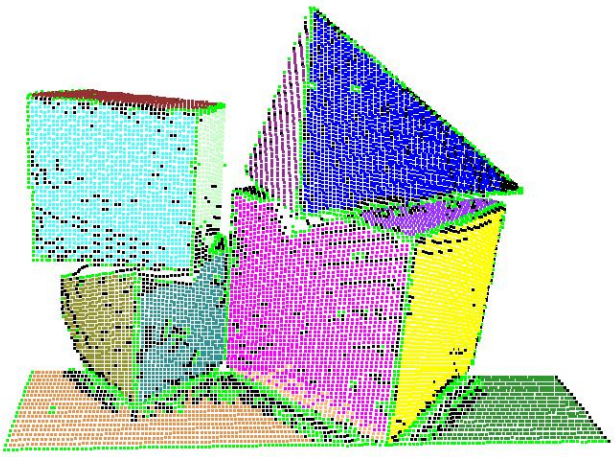

Figure 8. Planar surface segmentation of a 3D discrete point cloud: the number of points is 12859, and they are segmented into thirteen planar surfaces whose points are in different colors, except for those colored in light green that are detected as edge points.

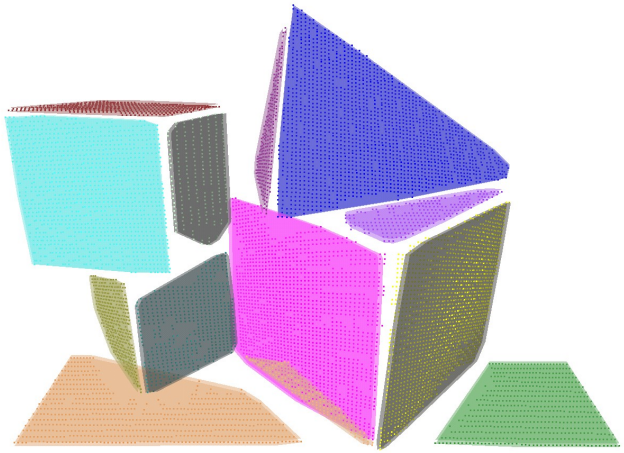

Figure 9. Fitted planes of segmented planar surface in Figure 8.

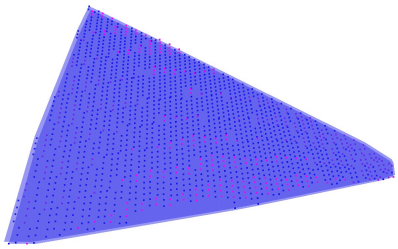

Figure 10. The fitted plane with its optimal consensus set for the blue segmented surface points in Figure 8: inliers are colored blue while outliers are colored pink.

Table 1. The number of points for each segmented surface in Figure 8 and the size of its optimal consensus set.

	Number of points	Opt. consensus set size
Blue	1770	1401
Yellow	1578	1195
Pink	1523	935
Pale Blue	1191	922
Orange	699	693
Green	573	573
Brown	545	544
Turquoise	536	512
Olive	440	405
Purple	248	245
Violet	232	206
Moss green	223	223
Cream	101	97

3D binary digital image. The first example is a 3D discrete point cloud in Figure 8, which is obtained after a planar surface segmentation of a range image of blocks [7]. The number of points in the cloud is 12859, and they are segmented into thirteen planar surfaces, which are illustrated in Figure 8 with points in different colors, except for those colored in light green that are detected as edge points. For each of these thirteen sets, we fitted a digital plane. We see the corresponding planes in Figure 9, and the number of points for each segmented surface and the size of its optimal consensus set in Table 1. In Figure 10, we also see that the fitted plane for the blue segmented surface points in Figure 8: inliers are colored blue while outliers are in pink.

We also applied our method to a 3D image extracted from a polymer foam observed in X-ray micro-tomography, on which homotopic thinning and surface decomposition were applied [11]. Figure 11 shows a cross section of the original image and Figure 12 shows a 3D binary image obtained after homotopic thinning and surface decomposition; the image is cut into two parts for visualization. Among around 400 sets of points forming surfaces in the entire image, we choose a part, as illustrated in Figure 13, including 17 decomposed surfaces for digital plane fitting. We show the fitted planes in Figure 14, and the number of points and the optimal consensus set size for each segmented surface in Table 2. For both the examples, we set $w = 1$.

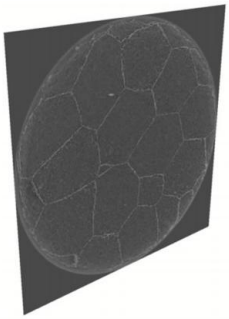

Figure 11. A cross section of a 3D image extracted from a polymer foam observed in X-ray micro-tomography.

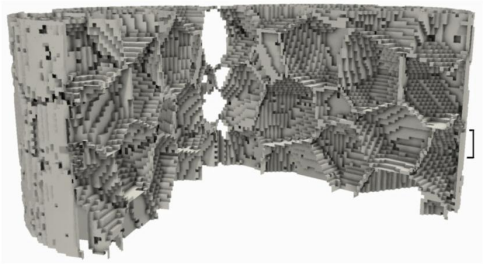

Figure 12. The 3D binary image obtained after homotopic thinning and surface decomposition applied on the image in Figure 11: the image is cut into two parts for visualization.

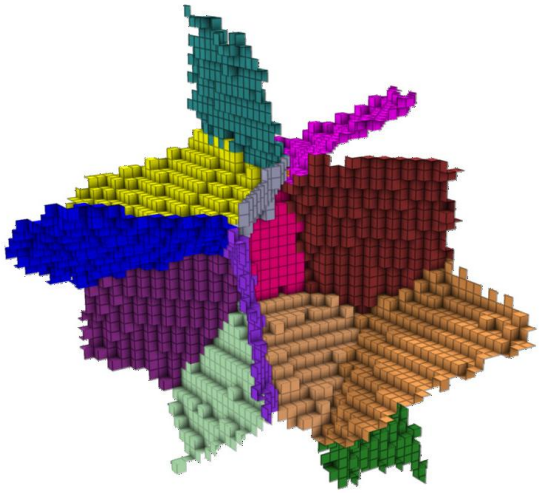

Figure 13. Selected decomposed surfaces, which is a part of the 3D binary image in Figure 12, for digital plane fitting.

7. Conclusions

In this paper we have exposed a new method for plane fitting on discrete data such as bitmap images and volumes, using a digital geometry (DG) approach. The DG approach allows practitioners to separate effects due to digitization on the one hand and noise on the other. Using our approach, we have proposed an optimal fitting method from the point of view of the maximal consensus set: we are guaranteed to fit discrete planes with the least amount of outliers.

Our algorithm has a complexity that are identical to parameter-less traditional plane-fitting algorithms such as least median of squares regression [14], but improves the detection of digital planes, in the presence of outliers. Future work will include improving algorithmic complexities and more complete applications such as optimal polyhedrization, image registration considering all feasible digital plane parameters.

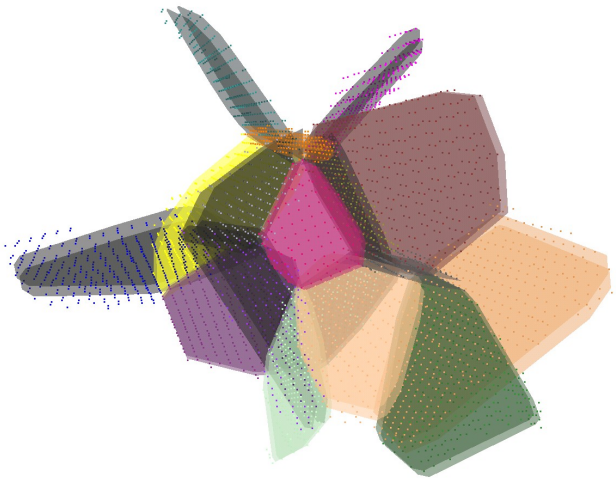

Figure 14. Fitted digital planes for decomposed surfaces shown in Figure 13.

Table 2. The number of points and the optimal consensus set size for each decomposed surface in Figure 14.

Number of points	Opt. consensus set size
541	269
512	233
439	208
427	196
427	200
405	208
377	159
335	206
333	169
309	141
308	168
258	76
220	104
200	90
198	61
163	98
104	71

Acknowledgement

The authors express their thanks to Mr. John Chaussard, who supplied the 3D image of decomposed surfaces extracted from a polymer foam used in the experiments. A part of this work has been supported by the French National Research Agency projects, ANR-05-BLAN-0071 (SURF) and BLAN07-2-184378 (MICROFISS).

References

[1] S. Boyd and L. Vandenberghe. *Convex optimization*. Cambridge University Press, 2004.

[2] C.-S. Chen, Y.-P. Hung, and J.-B. Cheng. A fast automatic method for registration of partially-overlapping range images. In *Proceedings of the VIth International Conference on Computer Vision*, pages 242–248, Bombay, 1998.

[3] M. de Berg, O. Cheong, M. van Kreveld, and M. Overmars. *Computational Geometry: Algorithms and Applications*. Springer-Berlag, Berlin Heidelberg, 2008.

[4] M. Fischler and R. Bolles. Random sample consensus: a paradigm for model fitting with applications to image analysis and automated cartography. *Communications of the ACM*, 24(6):381–395, 1981.

[5] Y. Garard, F. Feschet, and D. Coeurjolly. Gift-wrapping based preimage computation algorithm. In *Proceedings of International Conference on Discrete Geometry for Computer Imagery*, volume LNCS 4992, pages 310–321, 2008.

[6] R. Hartley and A. Zisserman. *Multiple view geometry in computer vision*. Cambridge University Press, 2003.

[7] Y. Kenmochi, L. Buzer, A. Sugimoto, and I. Shimizu. Discrete plane segmentation and estimation from a point cloud using local geometric patterns. *International Journal of Automation and Computing*, 5(3):246–256, 2008.

[8] C. Kim and I. Stojmenvić. On the recognition of digital planes in three-dimensional space. *Pattern Recognition Letters*, 12:665–669, 1991.

[9] R. Klette and A. Rosenfeld. *Digital Geometry: Geometric Methods for Digital Picture Analysis*. Morgan Kauffmann, San Francisco, 2004.

[10] K. Köster and M. Spann. Mir: An approach to robust clustering - application to range image segmentation. *IEEE Transactions on Pattern Analysis and Machine Intelligence*, 22(5):430–444, 2000.

[11] E. Plougonven, D. Bernard, and P. Viot. Quantitative analysis of the deformation of polypropylene foam under dynamic loading. *Progress in biomedical optics and imaging*, 7(38), 2006.

[12] W. Press, S. Teukolsky, W. Vetterling, and B. Flannery. *Numerical recipes: the art of scientific computing*. Cambridge University Press, third edition edition, 2007.

[13] L. Provot, L. Buzer, and I. Debled-Rennesson. Recognition of blurred pieces of discrete planes. In *Proceedings of International Conference of Discrete Geometry for Computer Imagery*, volume LNCS 4245, pages 65–76. Springer-Verlag, 2006.

[14] P. Rousseeuw. Least median of squares regression. *Journal of the American statistical association*, 79(388):871–880, 1984.

[15] H.-Y. Shum, K. Ikeuchi, and R. Reddy. Principal component analysis with missing data and its application to polyhedral object modeling. *IEEE Transactions on Pattern Analysis and Machine Intelligence*, 17(9):854–867, 1995.

[16] I. Sivignon, F. Dupont, and J.-M. Chassery. Decomposition of a three-dimensional discrete object surface into discrete plane pieces. *Algorithmica*, 38:25–43, 2004.

[17] R. Zrour, Y. Kenmochi, H. Talbot, L. Buzer, Y. Hamam, I. Shimizu, and A. Sugimoto. Optimal consensus set for digital line fitting. 2009. to appear in the 13th International Workshop on Combinatorial Image Analysis.